Aging Cell (2008) **7**, pp717–732 Doi: 10.1111/j.1474-9726.2008.00425.x

Partial proteasome inhibition in human fibroblasts triggers accelerated M1 senescence or M2 crisis depending on p53 and Rb status

Niki Chondrogianni,[1] Ioannis P. Trougakos,[1] Dimitris Kletsas,[2] Qin M. Chen[3] and Efstathios S. Gonos[1]

[1]National Hellenic Research Foundation, Institute of Biological Research and Biotechnology, Athens 11635, Greece
[2]National Center of Scientific Research Demokritos, Institute of Biology, Laboratory of Cell Proliferation and Aging, Athens 15310, Greece
[3]Department of Pharmacology, University of Arizona, Tucson, AZ 85724, USA

Summary

Proteasome-dependent degradation has been extensively investigated and has been shown to play a vital role in the maintenance of cellular homeostasis. Proteasome activity and expression are reduced during aging and replicative senescence. Its activation has been shown to confer lifespan extension in human diploid fibroblasts (HDFs), whereas partial proteasome inhibition triggers an irreversible premature senescent state in young HDFs. As p53 and Rb tumor suppressors regulate both replicative and premature senescence (RS and PS, respectively), in this study we investigated their implication in proteasome inhibition-mediated PS. By taking advantage of a variety of HDFs with defective p53 or/and Rb pathways, we reveal that proteasome activity inhibition to levels normally found in senescent human cells results in immediate growth arrest and/or moderate increase of apoptotic death. These effects are independent of the cellular genetic context. However, in the long term, proteasome inhibition-mediated PS can only be initiated and maintained in the presence of functional p53. More specifically, we demonstrate that following partial proteasome inhibition, senescence is dominant in HDFs with functional p53 and Rb molecules, crisis/death is induced in cells with high p53 levels and defective Rb pathway, whereas stress recovery and restoration of normal cycling occurs in cells that lack functional p53. These data reveal the continuous interplay between the integrity of proteasome function, senescence and cell survival.

Correspondence
Efstathios S. Gonos, National Hellenic Research Foundation, Institute of Biological Research and Biotechnology, 48 Vas. Constantinou Ave., Athens 11635, Greece. Tel.: +30 210 7273756; fax: +30 210 7273677; e-mail: sgonos@eie.gr

Accepted for publication *14 July 2008*

Key words: aging; premature senescence; proteasome; proteasome inhibition; p53; Rb.

Introduction

Human diploid fibroblasts (HDFs) undergo a limited number of divisions in culture and progressively, due to telomere shortening, reach a state of irreversible growth arrest, a process termed 'replicative senescence' (RS) or 'mortality stage 1' (M1) (Shay & Wright, 2005). Senescent fibroblasts exhibit several morphological and biochemical alterations as compared to their young/proliferating counterparts (Collado *et al*., 2007). Cells can transiently escape from senescence by interfering with p53 and retinoblastoma (Rb) tumor suppressor pathways, the two main regulatory axes of senescence progression (Ben-Porath & Weinberg, 2005). Once these pathways become inactivated, cells perform a significantly increased number of population doublings, reaching eventually a second proliferative lifespan barrier, termed 'crisis' or 'mortality stage 2' (M2). M2 is mainly characterized by extensive cell death rather than growth arrest (Shay & Wright, 2005). Senescence can be also accelerated by various factors. Three distinct types of premature senescence (PS) have been already reported: oncogene-induced PS (Serrano *et al*., 1997), oxidative stress-induced PS (Chen *et al*., 1998) and PS due to inhibition of important cellular pathways like proteasome-mediated degradation (Chondrogianni *et al*., 2003; Chondrogianni & Gonos, 2004). These findings have led to a distinction between RS, a term referring to senescence occurring after extended proliferation mainly triggered by cell-intrinsic mechanisms, and 'stress-induced premature senescence', a term referring to accelerated senescence mainly triggered by extrinsic factors (Shay & Wright, 2005). Although the molecular mechanisms regarding the two former types of PS are well characterized (Chen *et al*., 1998; Barradas *et al*., 2002), the signaling pathways involved in proteasome inhibition-mediated PS remain unknown.

p53 and Rb pathways are activated at distinct time points upon entry into senescence. Specifically, p53 protein is stabilized and differentially regulates its transcriptional targets (Oren, 2003); with $p21^{Cip1/WAF1}$ (hereafter referred to as p21) being the best characterized example of transactivation related to senescence induction (el-Deiry, 1998). On the other hand, $p105^{Rb}$ protein is found in its hypophosphorylated form in terminally senescent cells (Stein *et al*., 1999, and references therein) forbidding traverse through G1/S checkpoint via binding to the E2F protein family members, thus resulting in the subsequent repression of their transcriptional targets (Khidr

Aging Cell

& Chen, 2006). Phosphorylation of $p105^{Rb}$ and other cell cycle regulators is dependent on cyclin/cdk complexes and their inhibitors that are grouped in (i) $p16^{INK4a}$ (hereafter referred to as p16), $p15^{INK4b}$, $p18^{INK4c}$ and $p19^{INK4d}$ proteins which are members of the INK4 family that specifically inhibit the catalytic subunits of cdk4 and cdk6 kinases, and (ii) p21, $p27^{Kip1}$ (hereafter referred to as p27) and $p57^{Kip2}$ proteins which are members of the Cip/Kip family that affect the activities of cyclin D-, E- and A- dependent kinases (Sherr & Roberts, 2004).

Abrogation of p53 and Rb function has been achieved by mutations, deletions as well as by various DNA tumor viruses, such us the human papillomaviruses (HPV) and their E6 and E7 oncogene products. E6 is a viral E3 ligase that targets p53 protein for proteasome degradation (Münger & Howley, 2002). p53 abrogation in HDFs allows escape from M1 barrier by approximately 20 population doublings until cells reach a second proliferation barrier that closely resembles M1 (Bond *et al*., 1999). In contrast, E7 oncoprotein binds to all Rb family members ($p105^{Rb}$, p107 and p130) and disrupts Rb/E2F complexes, resulting in increased expression of E2F-responsive genes and consequent relief of S phase progression inhibition (Münger & Howley, 2002). Furthermore, E7 induces rapid proteasome degradation of hypophosphorylated Rb family members (Münger & Howley, 2002) and permits clonal expansion that is eventually limited by increased cell death, resulting in an M2-like state (Bond *et al*., 1999).

Proteasome-mediated protein degradation is an essential intracellular pathway, responsible for the regulation of homeostasis and survival. The proteasome is a cellular protease implicated in the removal of abnormal, denatured or otherwise damaged proteins and in the regulated degradation of short-lived proteins (Ciechanover, 2005; Goldberg, 2007). Alterations in proteasome function have been found in many biological processes including aging. We and others (reviewed in Chondrogianni & Gonos, 2005) have shown that the proteasome exerts a crucial role in the progression of aging and RS, involving partial loss of function upon aging of several human tissues as well as in senescent primary cultures. Additionally, we have demonstrated that upon its partial inhibition in young HDFs an irreversible, PS program is triggered (Chondrogianni *et al*., 2003; Chondrogianni & Gonos, 2004). In the current study, we provide direct evidence that p53 mainly regulates proteasome inhibition-mediated PS.

Results

Partial proteasome inhibition, to levels found in senescent HDFs, triggers PS in young cells with functional p53

As in previous studies we have shown PS induction following partial proteasome inhibition in young HDFs (Chondrogianni *et al*., 2003; Chondrogianni & Gonos, 2004), in this work we aimed to decipher the molecular events that underlie this phenomenon. To this end, initially, we took advantage of three genetically altered IMR90 cell lines – namely, IMR90/E6, IMR90/E7 and IMR90/E6E7 cells (hereafter referred to as E6, E7 and E6E7) – defective in p53, Rb and both oncosuppressor proteins, respectively. These cell lines exhibit similar levels of chymotrypsin-like (CT-L) activity, expression of proteasome subunits and levels of oxidized proteins (Table 1 and Fig. S1). Treatment with 10 nM epoxomicin, a highly specific and irreversible proteasome inhibitor, for 4 days yielded approximately a 50% inhibition of the proteasomal CT-L activity in all cell lines [Table 1; CT-L remaining activity (%)] in accordance with previous data (Chondrogianni *et al*., 2003). We then examined the long-term effects of partial proteasome inhibition on the proliferative capacity and physiology of the corresponding cell lines [results obtained for parental IMR90 and empty vector infected cells were similar, thus they are presented here as control (CON)].

Table 1 Proteasome inhibition effects on CON, E7, E6 and E6E7 cells depend on both the extent of inhibition of proteasome activity and the cellular context

		CT-L relative activity (%)			
Epoxomicin concentration	CT-L remaining activity (%)	CON 100.0 ± 1.2	E7 112.9 ± 1	E6 104.2 ± 7.1	E6E7 105.1 ± 7.8
0 nM (DMSO)	100.0 ± 2.7	Normal proliferation	Normal proliferation	Normal proliferation	Normal proliferation
5 nM	89.0 ± 3.2	Normal proliferation	Normal proliferation	Normal proliferation	Normal proliferation
10 nM	52.0 ± 2.3	Premature senescence	Premature senescence/death	Resumption of growth	Resumption of growth
20 nM	43.0 ± 1.2	Premature senescence	Death	Resumption of growth	Resumption of growth
30 nM	30.0 ± 2.8	Premature senescence/death	Death	Resumption of growth	Resumption of growth
50 nM	7.3 ± 0.15	Death	Death	Death	Resumption of growth

Percentage of the relative CT-L activity among the different cell lines as well as of the remaining CT-L activity following treatment with epoxomicin concentrations ranging from 5 nM to 50 nM in CON, E7, E6 and E6E7 cell lines (second column). Mean value of activity in each DMSO-treated cell line was set at 100%. The experiment was performed twice and ± denotes SE. Phenotypic responses following epoxomicin withdrawal and cell recovery were recorded (columns 3–6) and referred to as *normal proliferation* when cells were not affected by the inhibitor, *premature senescence* when cells entered irreversible PS, *premature senescence/death* when cells initially exhibited a stress-induced growth arrest and then became apoptotic, *resumption of growth* when cells restarted proliferation after a stress-related growth arrest and *death* when cells died in the presence of the inhibitor.

As expected, epoxomicin-treated CON cells ceased proliferation and acquired prematurely a senescent morphology (Fig. 1A). Interestingly, epoxomicin effects varied significantly on the other cell lines. Epoxomicin-treated E7 cells showed no increase of their cell number at the end of the treatment (Epox/4d+0). After this point the cell cultures rapidly deteriorated and no cells survived after 3 weeks (Epox/4d+3wk). In contrast, epoxomicin-treated E6 and E6E7 cells, after an initial retardation of proliferation (Epox/4d+0), resumed normal growth following inhibitor withdrawal. Epoxomicin-treated E6E7 cells resumed growth in a more aggressive manner as compared to E6 cells. Similar results were obtained when cells were exposed to MG132, a reversible proteasome inhibitor (Chondrogianni & Gonos, 2004), thus excluding the possibility of an epoxomicin-specific effect (data not shown).

We then tested the cultures for known features of senescence. Epoxomicin-treated CON cells exhibited the typical senescent morphology 1 week after epoxomicin withdrawal (Fig. 1B) and more than 90% of the cells stained positively for β-galactosidase activity, a marker of senescence, 2 weeks later (Fig. 1C). Epoxomicin-treated E7 cells acquired a senescent morphology and were almost 100% β-galactosidase positive 2 weeks after epoxomicin removal. In contrast, epoxomicin-treated E6 and E6E7 cultures resumed growth and retained their 'young' morphology following inhibitor withdrawal (Fig. 1B) with low numbers of β-galactosidase-positive cells (Fig. 1C).

Given that high concentrations of proteasome inhibitors have been reported to increase intracellular reactive oxygen species (ROS) levels (Kikuchi *et al*., 2003), we checked whether this also occurs under our experimental conditions. Measurement of ROS levels immediately after epoxomicin treatment did not reveal any significant elevation (Fig. 1D; Epox/4d+0), a finding also supported by the lack of significantly accumulated oxidized proteins at this time point (Chondrogianni *et al*., 2003). However, when the final state was established (after 2 weeks for CON cells and 1 week for E7 cells), CON and E7 cells that prematurely senesced exhibited increased intracellular ROS levels. No significant increases of ROS levels were detected in E6 and E6E7 cells that resumed growth (data not shown). To analyze ROS implication in proteasome inhibition-mediated PS, we co-treated the cells with epoxomicin and the antioxidant N-acetyl-cysteine (NAC). We found that NAC could not rescue CON or E7 cells from PS. Interestingly, proteasome inhibition-mediated PS was delayed by approximately 2 weeks in NAC-treated CON and E7 cells, whereas E6 and E6E7 cells resumed normal growth faster. Upon establishment of the final cellular state increased ROS levels were also recorded (in CON cells), albeit at lower levels as compared to the cells that were not co-incubated with NAC (Fig. 1D). Thus, although elevated ROS levels may contribute to the establishment of proteasome inhibition-mediated PS, they appear to be a late outcome of the treatment since we did not detect increased ROS levels immediately after epoxomicin treatment (Epox/4d+0). Consistent with this, there was a slight increase of the phosphorylation of the redox-sensitive protein kinase p38, that will have to be addressed in future work (Fig. S2).

Regarding the molecular axis involved in proteasome inhibition-mediated PS execution, our data suggested that it is p53 dependent. To verify this assumption we assayed the effects of proteasome inhibition in TR9-7 fibroblasts that conditionally express p53 (Agarwal *et al*., 1995). Exposure of TR9-7 cells to epoxomicin in the absence of p53 expression resulted in normal growth after epoxomicin removal (Fig. 2A,B; left panels). This was also the case for the parental MDAH041 cells (p53 null; data not shown). In contrast, parallel induction of p53 and cell exposure to epoxomicin for 4 days promoted PS (Fig. 2A) and a senescent morphology (Fig. 2B, right panels). These data provide strong evidence that induction of PS following partial proteasome inhibition in HDFs depends on functional p53.

Since it was shown that oncogene induced senescence involves activation of p53 via the DNA damage response (Di Micco *et al.*, 2006), we have checked for evidence of a DNA damage response in our experimental model. We detect neither phosphorylation of histone H2 (γ-H2AX) and chk1 (data not shown) nor any significant increase in the levels of phosphorylated p53 on Ser 15 (Lavin & Gueven, 2006) following partial epoxomicin treatment (Fig. S2). These data along with the observed lack of increase of ROS levels (Fig. 1D) immediately after treatment indicate the absence of a DNA damage response following partial proteasome inhibition.

'Lifespan program' execution is accelerated in cell lines with functional p53 following partial proteasome inhibition

Next, we studied the cell cycle distribution of all cell lines following partial proteasome inhibition during the entire experiment (Fig. 3). We observed an immediate increase in the percentage of cells in G2/M phase (Epox/4d+0) in all cell lines, ranging from ~1.8- to 2.1-fold for E7 and E6E7 cells, to ~3.1-fold for E6 cells and to ~10.8-fold for CON cells, as compared to DMSO-treated cells. However, the cell cycle distribution varied between different cells lines as cultures progressed during the experiment. Epoxomicin-treated CON cultures retained an increased percentage of G2/M phase cells (over 3-fold induction 3 weeks post-treatment). Interestingly, although S phase cells were reduced to 3.29% immediately after treatment (Epox/4d+0), they accumulated to 67.87% 1 week later (probably in an attempt to re-enter the cell cycle), and then decreased again. Regarding epoxomicin-treated E7 cells, no S phase cells were detected after epoxomicin treatment (Fig. 3). An accumulation of G2/M phase arrested cells was recorded 2 weeks post-treatment, before cell death occurred. To verify whether these findings reflect senescence state we also performed cell cycle analysis in CON and E7 cells that ceased proliferation in culture after serial passaging. Senescent CON and E7 cells exhibited similar cell cycle distributions to those recorded in their respective epoxomicin-treated cultures (data not shown). Finally, epoxomicin-treated E6 and E6E7 cells re-acquired their usual cell cycle profile after epoxomicin removal. Interestingly, E6E7 cells adopted normal cell cycle profile 1 week post-treatment

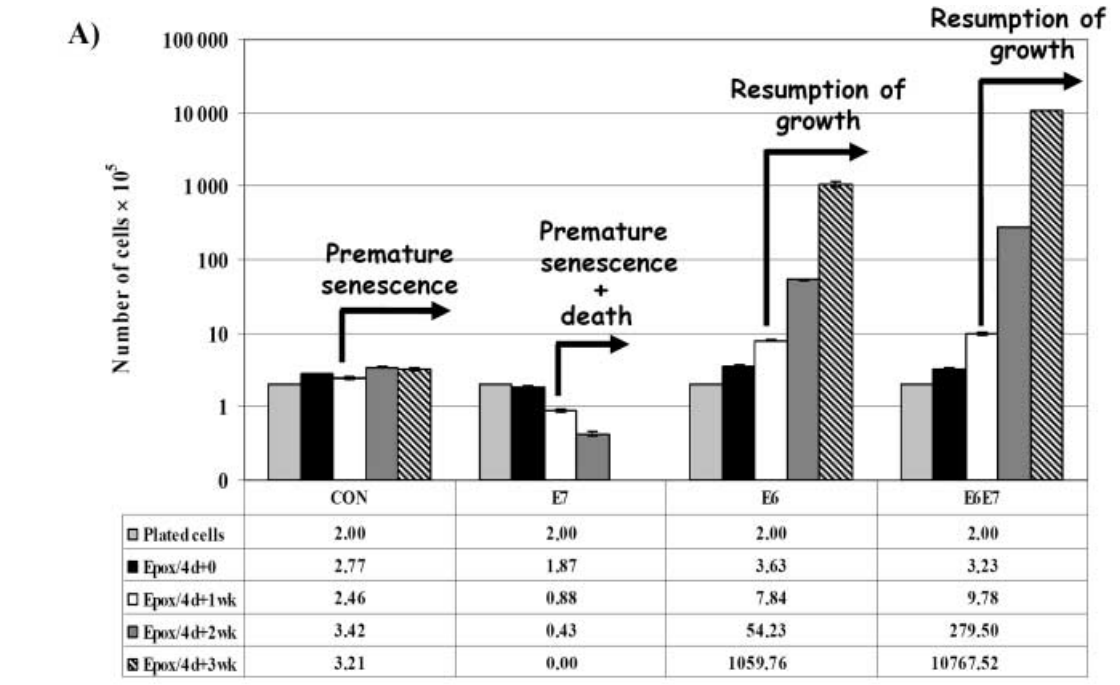

	CON	E7	E6	E6E7
Plated cells	2.00	2.00	2.00	2.00
Epox/4d+0	2.77	1.87	3.63	3.23
Epox/4d+1wk	2.46	0.88	7.84	9.78
Epox/4d+2wk	3.42	0.43	54.23	279.50
Epox/4d+3wk	3.21	0.00	1059.76	10767.52

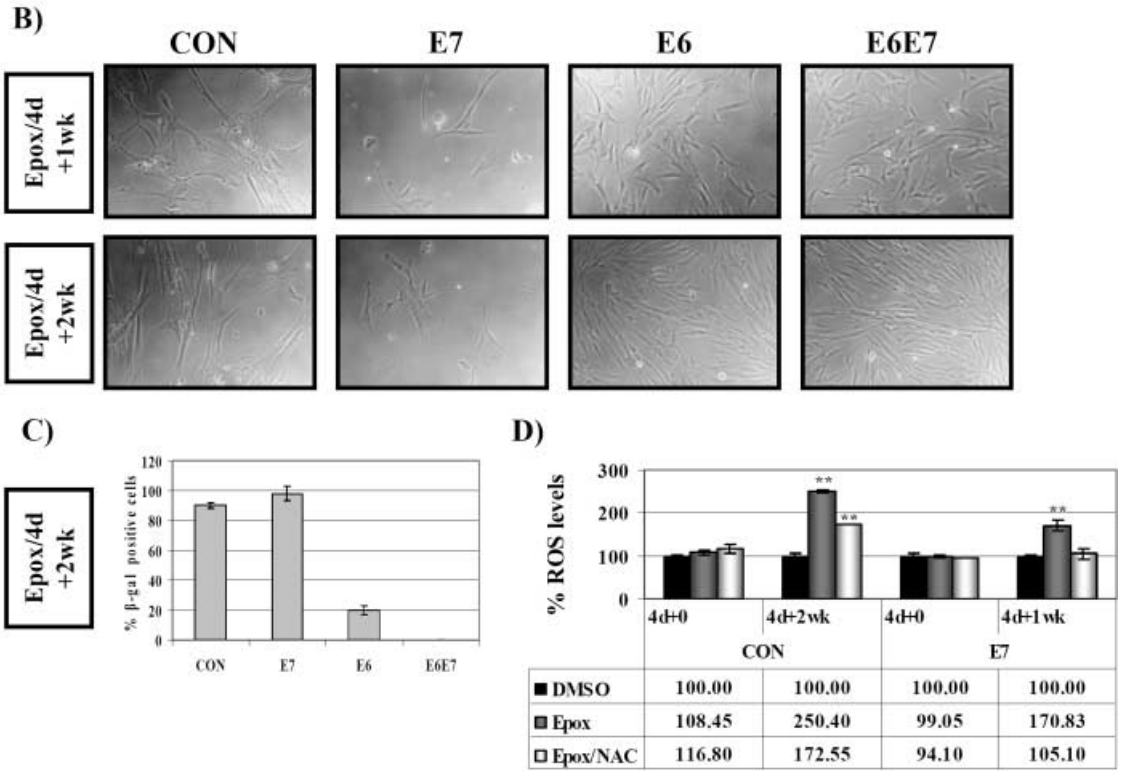

	CON		E7	
DMSO	100.00	100.00	100.00	100.00
Epox	108.45	250.40	99.05	170.83
Epox/NAC	116.80	172.55	94.10	105.10

Fig. 1 Effect of partial proteasome inhibition to CON, E7, E6 and E6E7 cells. (A) Number of CON, E7, E6 and E6E7 cells (× 10^5) exposed to 10 nM epoxomicin immediately (4d+0), 1 (4d+1wk), 2 (4d+2wk) and 3 (4d+3wk) weeks after inhibitor removal. Legends on the graph report the final observed state of each cell line. (B) Representative photos and (C) percentages of SA-β-galactosidase positive cells of epoxomicin-treated cell lines (B) 1 (4d+1wk) and (B, C) 2 (4d+2wk) weeks after epoxomicin treatment. (D) Percentages of ROS levels in CON and E7 cells exposed to 10 nM epoxomicin (± NAC) or DMSO immediately (4d+0), 1 (4d+1wk; for E7 cells) or 2 (4d+2wk; for CON cells) weeks after inhibitor removal. ROS levels of DMSO-treated cells at each time point were arbitrary set to 100%. Error bars denote ± standard error.

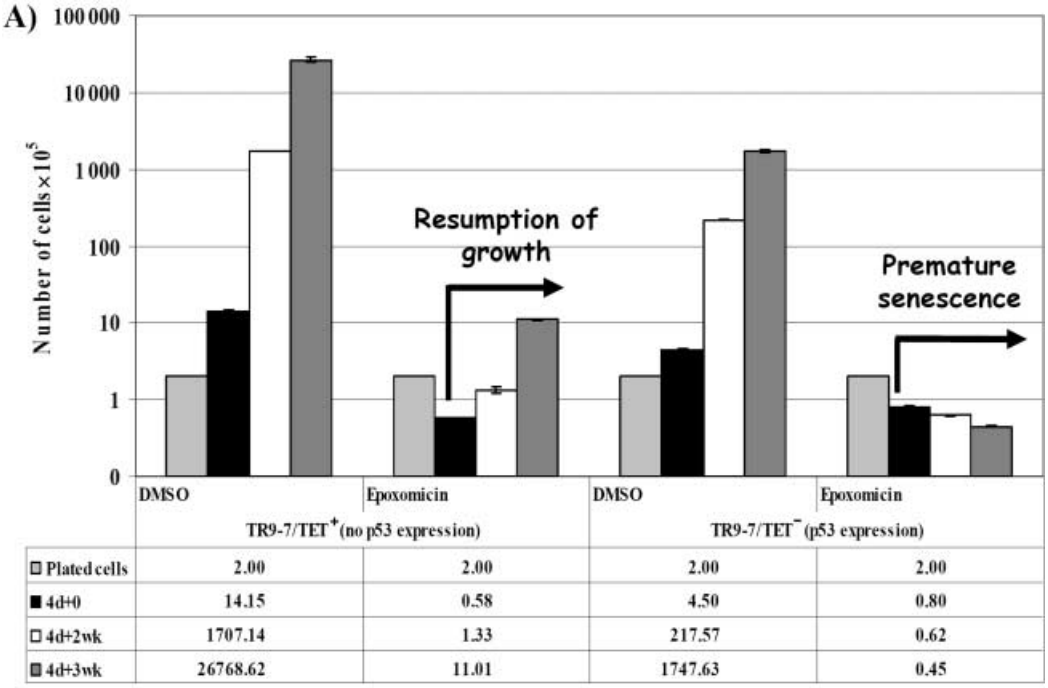

	TR9-7/TET+ (no p53 expression)		TR9-7/TET− (p53 expression)	
	DMSO	Epoxomicin	DMSO	Epoxomicin
Plated cells	2.00	2.00	2.00	2.00
4d+0	14.15	0.58	4.50	0.80
4d+2wk	1707.14	1.33	217.57	0.62
4d+3wk	26768.62	11.01	1747.63	0.45

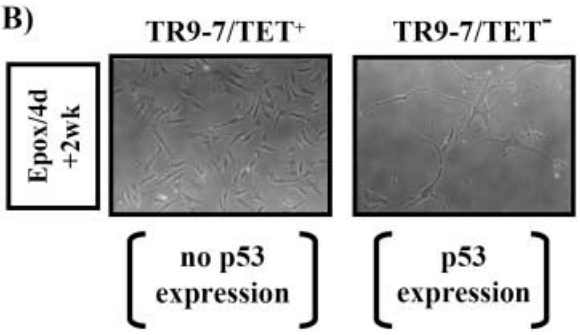

Fig. 2 Effect of partial proteasome inhibition in TR9-7 cells. (A) Number (× 10^5) of TR9-7/TET$^+$ (no p53 expression) and TR9-7/TET$^-$ (p53 expression) cells exposed to 10 nM epoxomicin or DMSO immediately (4d+0), 2 (4d+2wk) and 3 (4d+3wk) weeks after inhibitor removal. Legends on the graph report the final observed state of each cell line. Error bars denote ± standard error. (B) Representative photos of epoxomicin-treated cell lines 2 weeks (4d+2wk) after epoxomicin treatment.

whereas E6 cells resumed normal growth 2 weeks post-treatment (Fig. 3). In conclusion, these results suggest that inhibition of proteasome activity in young HDFs with functional p53 (CON and E7 cells) to levels found in senescent HDFs results in an accelerated execution of their lifespan program, i.e. PS for CON cells and PS/crisis for E7 cells. In contrast, HDFs with defective p53, like E6 and E6E7 cells, despite an initial arrest at G2/M phase, escape from this accelerated execution of lifespan progression. Thus, functional p53 is essential in proteasome inhibition-mediated PS establishment.

Next we proceeded to the analysis of the molecular basis of these cellular alterations. First, we examined the protein expression levels of p53 and p105^{Rb} following proteasome inhibition. As shown in Fig. 4A1, basal p53 levels were higher in E7 cells as compared to CON cells in agreement with previously reported data (Chen *et al*., 1998). Moreover, p53 accumulated in both CON and E7 cells following epoxomicin treatment (Epox/4d+0); these increased p53 levels were maintained throughout the experiment. No p53 was detected in E6 and E6E7 cells, presumably due to its E6-mediated degradation. p105^{Rb} hypo- and hyper- phosphorylated levels were higher in E6 cells as compared to CON cells (Chen *et al.*, 1998; Malanchi *et al.*, 2004), whereas, E7 and E6E7 cells possessed decreased levels due to the E7-induced degradation (Münger & Howley, 2002). p105^{Rb} was mainly found in its hypophosphorylated form in epoxomicin-treated CON cells and, more importantly, it was further down-regulated as cells progressed to senescence. In contrast, we did not observe any significant changes of p105^{Rb} expression in epoxomicin-treated E6 and E6E7 cells. Regarding the other Rb-family members, no significant changes were recorded (data not shown). We also observed up-regulation of GRP78/BiP protein, a marker of endoplasmic reticulum (ER) stress

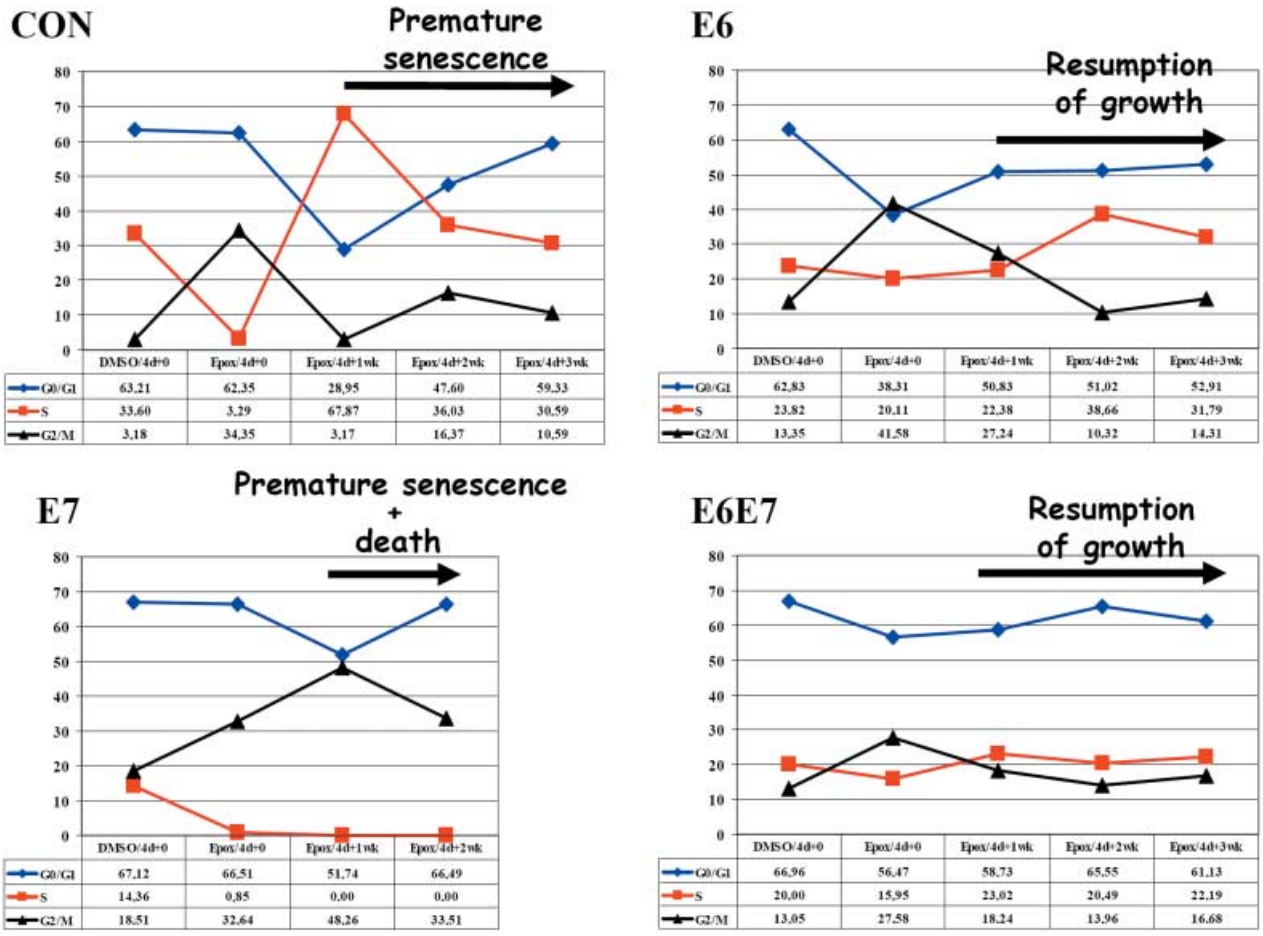

Fig. 3 Cell cycle distribution analysis of CON, E7, E6 and E6E7 cells following partial proteasome inhibition. Flow cytometry analysis of CON, E7, E6 and E6E7 cells exposed to 10 nM epoxomicin or DMSO immediately (4d+0), 1 (4d+1wk), 2 (4d+2wk) and 3 (4d+3wk) weeks after inhibitor removal. Analysis for E7 cells was performed up to the 2nd week only, due to massive cell death after that time point. Graphs depict cell percentage in each phase of the cell cycle. Arrows and legends on the graphs indicate the point where each final state is predominantly established.

(Oyadomari & Mori, 2004), as well as of GADD153 in all epoxomicin-treated cell lines (Epox/4d+0, Fig. 4A2). ER stress is a known feature of proteasome inhibition (Patil & Walter, 2001) that has been associated with a G2/M shift in yeast (Fleming *et al.*, 2002; Bonilla & Cunningham, 2003). Similarly, GADD153 is induced in G2/M growth arrested cells (Hollander & Fornace, 2002; Oyadomari & Mori, 2004). These data further explain the observed G2/M phase cell shift following epoxomicin treatment and suggest that this arrest is p53 and Rb independent.

We then analyzed several cell cycle regulators (Fig. 4A3). Proteins that permit G1/S transition, like cyclin A and proliferating cell nuclear antigen (PCNA), were down-regulated in epoxomicin-treated CON cells. In contrast, negative regulators of cell cycle progression like p16, p21 and p27 were found to accumulate in the same cells albeit at different kinetics. More precisely, p21 protein was increased at the end of the treatment (Epox/4d+0) consistent with p53 accumulation (Fig. 4A1), followed by a down-regulation during the following weeks. In parallel, p27 also accumulated, indicative of S phase progression inhibition. Finally, p16 massively accumulated during the 1st and the 2nd week post-treatment. The kinetics of p16 expression most probably ensured growth arrest maintenance in CON cells. M phase-related proteins, like cdk1 and cyclin B1, were decreased, in agreement with the observed G2/M arrest. Hence, the protein expression profile in CON cells advocates for the launch of PS. In contrast, positive cell cycle regulators were not altered or were even increased in E6 and E6E7 cells in accordance with their elevated proliferative rates. Additionally, levels of mitosis promoting factors (such as cdk1 and cyclin B1) were almost not affected, thereby participating in the restoration of normal growth. Finally, in epoxomicin-treated E7 cells we found accumulation of both promoters (like PCNA) and negative regulators of G1/S progression, like p21, p27 and p16. Accordingly, after epoxomicin removal (Epox/4d+0), M phase-associated proteins (cyclin B1 and cdk1) were down-regulated and their expression was restored during the recovery period (Epox/4d+1wk). These data, in combination with the diminishing cell numbers (see Fig. 1A), suggest that the end point of epoxomicin-treated E7 cells is most probably characterized by crisis/death. Although additional analysis is needed, it is likely that this occurs during S phase

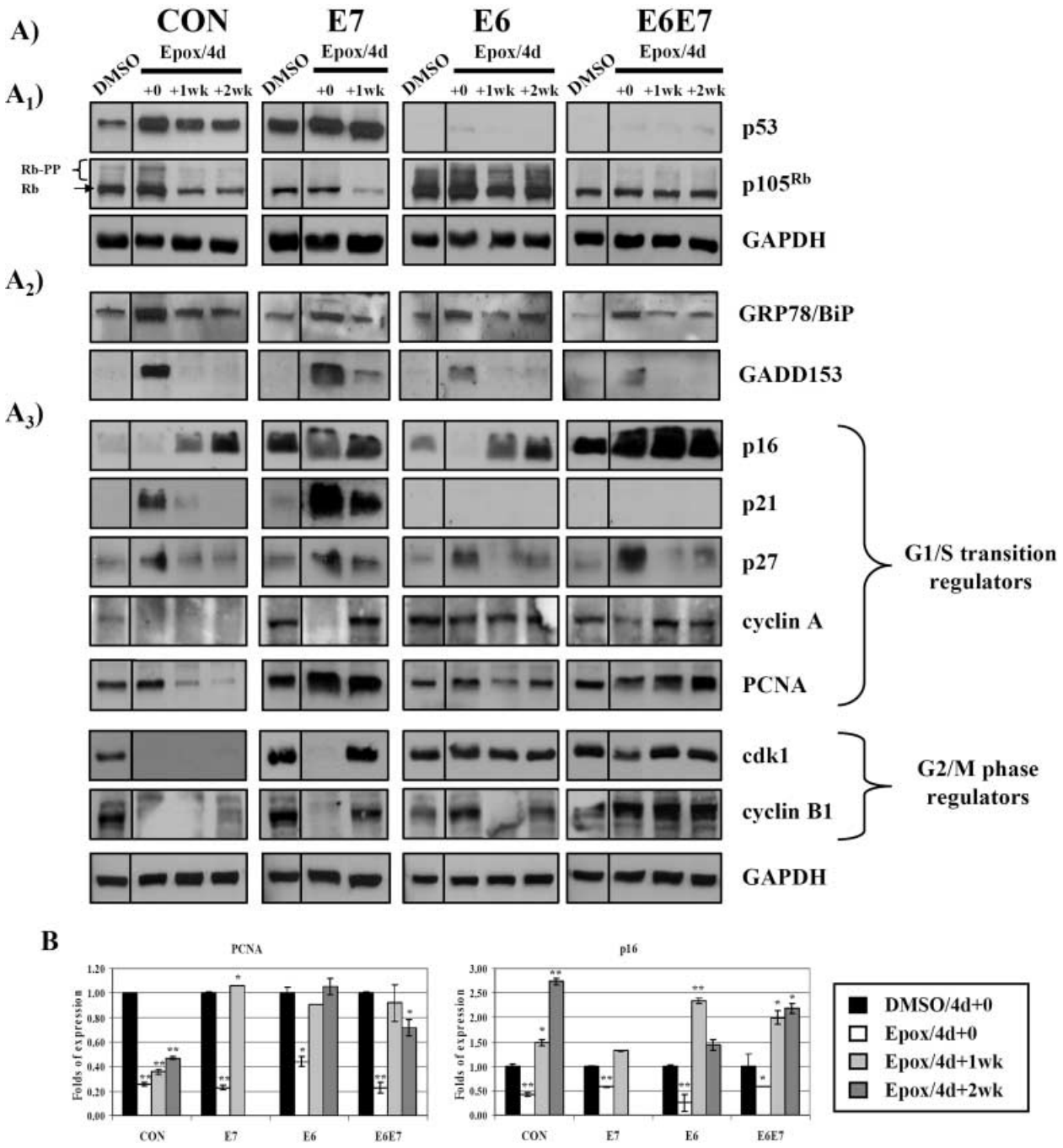

Fig. 4 Protein and RNA expression levels of cell cycle regulators in CON, E7, E6 and E6E7 cells following partial proteasome inhibition. (A) Immunoblot analysis of (A1) p53 and p105^{Rb} proteins, (A2) GRP78/BiP and GADD153 proteins, (A3) regulators related to G1/S transition [p16, p21, p27, cyclin A and PCNA] and G2/M phases [cdk1 and cyclin B1] in CON, E7, E6 and E6E7 cells exposed to 10 nM epoxomicin or DMSO immediately (4d+0), 1 (4d+1wk) and 2 (4d+2wk) weeks after inhibitor removal. (B) Real-time PCR analysis of PCNA and p16 genes in CON, E7, E6 and E6E7 cells exposed to 10 nM epoxomicin or DMSO immediately (4d+0), 1 (4d+1wk) and 2 (4d+2wk) weeks after inhibitor removal. Equal protein loading was verified by reprobing the membranes with a GAPDH antibody. Rb and Rb-PP denote the hypo- and hyper-phosphorylated forms of p105^{Rb}. Expression level of each gene was arbitrary set to 1 in respective control cultures (DMSO-treated) of each time point. Error bars denote ± standard error.

while cells attempt to progress through DNA replication in order to restore their normal cell cycling. This assumption is further supported by our finding of elevated S phase related proteins with a parallel absence of S phase cells.

Since most of the examined cell cycle regulators are proteasome substrates, we also aimed to address whether their protein accumulation is attributed solely to the inhibition of proteolysis. Representative examples of RNA expression levels for PCNA and

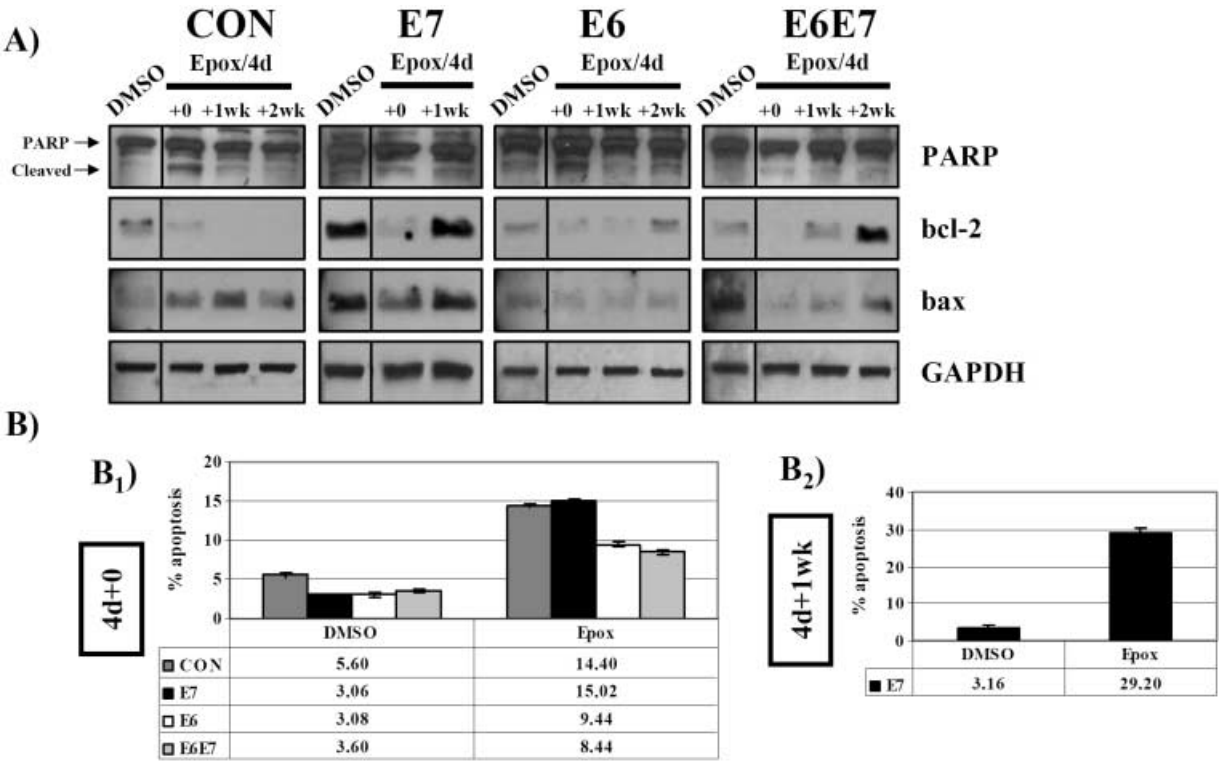

Fig. 5 Cell death analysis in CON, E7, E6 and E6E7 cells following partial proteasome inhibition. (A) Immunoblot analysis of PARP, bcl-2 and bax proteins in CON, E7, E6 and E6E7 cells exposed to 10 nM epoxomicin or DMSO immediately (4d+0), 1 (4d+1wk) and 2 (4d+2wk) weeks after inhibitor removal. The 85 kDa apoptotic fragment of PARP is indicated as 'cleaved'. Analysis for E7 cells was performed up to the 1st week. Equal protein loading was verified by reprobing the membranes with a GAPDH antibody. (B) Percentage of subdiploid events as recorded by flow cytometry analysis of (B1) CON, E7, E6 and E6E7, and (B2) E7 cells exposed to 10 nM epoxomicin or DMSO (B1) immediately (4d+0) or (B2) 1 (4d+1wk) week after inhibitor removal.

p16 genes are presented in Fig. 4B. PCNA protein accumulated at the end of treatment (Epox/4d+0), despite the decrease of its RNA expression levels (compare data in Fig. 4A3 and Fig. 4B), arguing for the significance of the deregulated proteasome-mediated degradation. However, during the following weeks, after the relief of proteasome inhibition, PCNA protein levels eventually matched the RNA expression levels. In contrast, p16 protein levels appeared to follow the RNA expression profile throughout the experiment. Thus, the observed changes in the protein expression profiles can be attributed to both alterations of gene transcription and partial inhibition of protein degradation.

Partial proteasome inhibition-mediated cell death in HDFs is independent of the p53/Rb status

Since it is known that proteasome inhibition triggers apoptosis (Wojcik, 1999), we then studied the levels of cell death under our experimental conditions. The C-terminal 85 kDa apoptotic fragment of poly ADP-ribose polymerase (PARP) which is indicative of ongoing apoptosis was detected in all cell lines immediately after epoxomicin treatment (Epox/4d+0; Fig. 5A). Additionally, bcl-2 was down-regulated and bax was up-regulated resulting in altered bcl-2/bax ratio. In support, flow cytometric analysis of the subdiploid fraction verified the increased levels of apoptosis in all cell lines at the same time point (Fig. 5B1). However, following epoxomicin withdrawal no apoptosis was detected, except for E7 cells that continued dying as shown by flow cytometry analysis in Fig. 5B2. In summary, cell death induction after partial proteasome inhibition in HDFs does not solely relate to p53 or Rb.

Partial proteasome inhibition in HDFs triggers a common immediate cellular response regardless of the p53 and Rb status

Next we investigated the molecular basis of the immediate effects of partial proteasome inhibition. First, we determined epoxomicin effects on cultures' proliferative capacities during the 4 days of treatment. As it is shown in Fig. 6A, all cell lines ceased proliferation on the 1st day of treatment. At day 4,

Fig. 6 Immediate effect of epoxomicin to CON, E7, E6 and E6E7 cells. (A) Number of CON, E7, E6 and E6E7 cells ($\times 10^5$) exposed to 10 nM epoxomicin for 1–4 days (1–4d) or DMSO (4d). Error bars denote ± SE (B) Representative photos of all cell lines after 4 days of epoxomicin treatment (Epox/4d). (C) Flow cytometry analysis of CON, E7, E6 and E6E7 cells exposed to 10 nM epoxomicin for 1–4 days (1–4d) or DMSO for 4 days (4d). Graphs depict cell percentage in each phase of the cell cycle.

A)

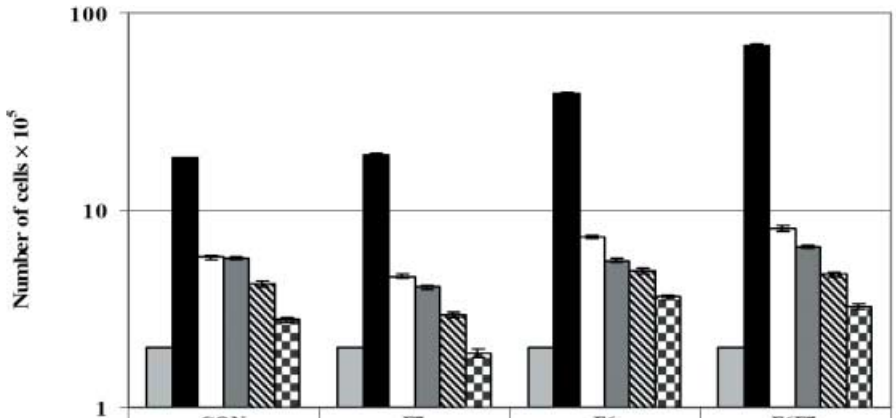

	CON	E7	E6	E6E7
Plated cells	2.00	2.00	2.00	2.00
DMSO/4d	18.31	19.04	38.94	68.08
Epox/1d	5.75	4.62	7.31	8.05
Epox/2d	5.67	4.07	5.55	6.53
Epox/3d	4.22	2.95	4.88	4.72
Epox/4d	2.77	1.87	3.63	3.23

B)

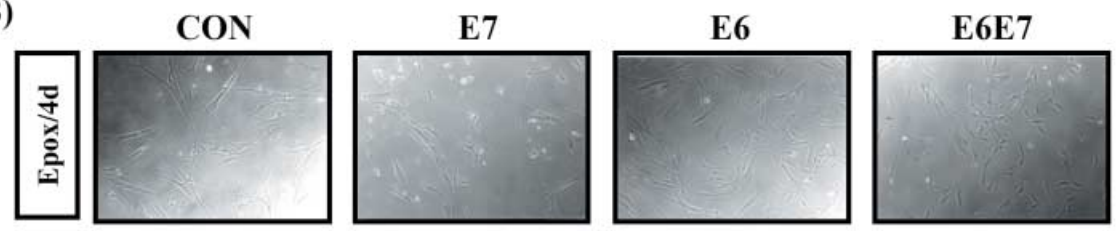

C)

CON

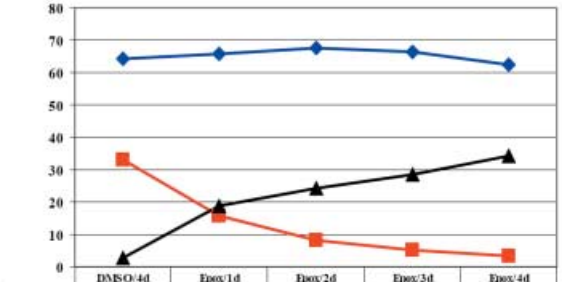

	DMSO/4d	Epox/1d	Epox/2d	Epox/3d	Epox/4d
G0/G1	64.28	65.61	67.63	66.37	62.35
S	33.08	15.71	8.08	5.22	3.29
G2/M	2.65	18.69	24.29	28.40	34.35

E6

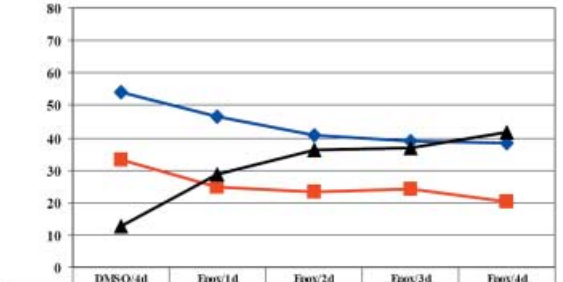

	DMSO/4d	Epox/1d	Epox/2d	Epox/3d	Epox/4d
G0/G1	54.07	46.56	40.63	38.90	38.31
S	33.23	24.65	23.12	24.19	20.11
G2/M	12.70	28.79	36.25	36.90	41.58

E7

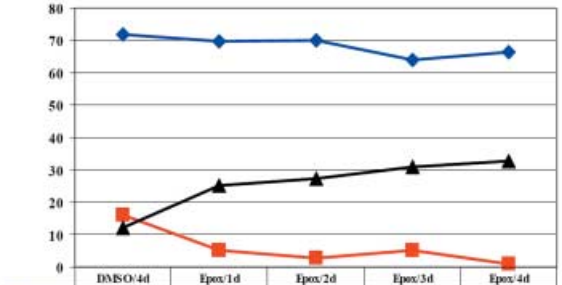

	DMSO/4d	Epox/1d	Epox/2d	Epox/3d	Epox/4d
G0/G1	71.92	69.72	70.00	63.89	66.51
S	15.96	5.19	2.58	5.19	0.85
G2/M	12.12	25.09	27.42	30.92	32.64

E6E7

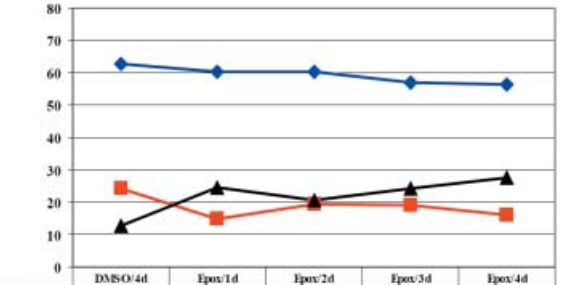

	DMSO/4d	Epox/1d	Epox/2d	Epox/3d	Epox/4d
G0/G1	62.78	60.34	60.16	56.82	56.47
S	24.38	14.98	19.38	19.05	15.95
G2/M	12.84	24.68	20.46	24.13	27.58

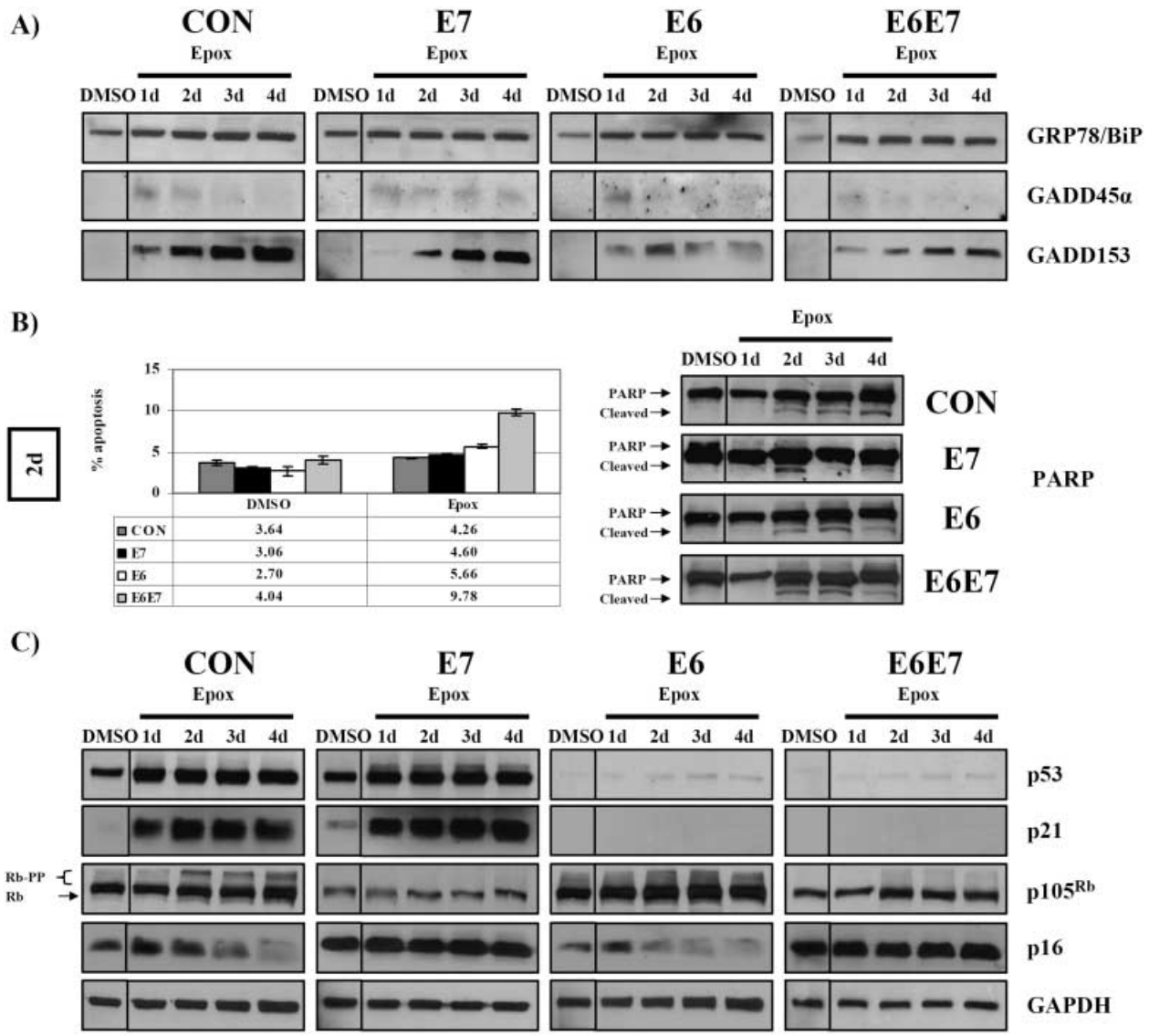

Fig. 7 Protein expression levels of cell cycle regulators in CON, E7, E6 and E6E7 cells during epoxomicin treatment. Immunoblot analysis of (A) GRP78/BiP, GADD45α and GADD153, (B, right panel) PARP, and (C) p53, p21, $p105^{Rb}$ and p16 proteins in CON, E7, E6 and E6E7 cells exposed to 10 nM epoxomicin or DMSO for 1–4 days (1–4d). Equal protein loading was verified by reprobing the membranes with a GAPDH antibody (Fig. 7C). Rb and Rb-PP denote the hypo- and hyper-phosphorylated forms of $p105^{Rb}$. The 85 kDa apoptotic fragment of PARP is indicated as 'cleaved'. (B, left panel) Percentage of subdiploid events as recorded by flow cytometry analysis of CON, E7, E6 and E6E7 cells exposed to 10 nM epoxomicin or DMSO for 2 days (2d).

~41% CON, ~30% E7, ~40% E6 and ~27% E6E7 epoxomicin-treated cells were found as compared to the numbers of the respective DMSO-treated cells at day 1 (DMSO/1d, data not shown). All epoxomicin-treated cells exhibited typical stress-fibers at day 1 (not shown). After 4 days of continuous exposure to epoxomicin, all cultures were stressed but treated CON and E7 cells were enlarged and flattened, whereas very few enlarged cells were detected in E6 and E6E7 cultures (Fig. 6B). We then determined the cell cycle distribution during the 4 days of treatment (Fig. 6C). A significant increase of G2/M phase cells along with a simultaneous decrease of S phase cells were observed for all cell lines. G2/M phase shift mainly occurred on the 1st day (Epox/1d) and it was more pronounced in CON cells where it reached a ~13-fold increase by the 4th day as compared to a ~2.2- to 3.3-fold increase in the other cell lines.

We also examined the protein expression levels of the ER-stress marker, GRP78/BiP, as well as the G2/M related proteins, GADD45α and GADD153 (Fig. 7A). All epoxomicin-treated cells exhibited an induction of GRP78/BiP during proteasome inhibition, a minimal up-regulation of GADD45α at day 1 which was diminished afterwards and finally a gradual induction of GADD153 which was more pronounced in CON and E7 cells. Flow cytometry analysis of the subdiploid fraction of epoxomicin-treated cell lines verified apoptosis initiation 48 h

after starting epoxomicin treatment (Fig. 7B, left panel). In accordance to this observation, PARP was cleaved to its C-terminal 85 kDa apoptotic fragment in all cell lines beginning at the 2nd day (Fig. 7, right panel), while bcl-2 protein levels decreased and bax levels increased, leading to a distortion of bcl-2/bax ratio (data not shown).

Finally, we investigated changes of the p53-p21 and Rb-p16 protein expression levels during the treatment. As shown in Fig. 7C, both p53, and its downstream target p21, proteins significantly accumulated in CON and E7 cells. A minimal accumulation of p53 was evident even in E6 and E6E7 cells, most probably due to the partial inhibition of proteasome-mediated degradation that was, however, insufficient to promote p21 up-regulation. Regarding $p105^{Rb}$, its hypo- and hyper-phosphorylated forms were slightly accumulated in CON and E6 epoxomicin-treated cells after 2 days of treatment. This could be either attributed to the partial restriction of proteasomal degradation or, with respect to the E6 cell line, to E6-mediated promotion of $p105^{Rb}$ phosphorylation (Malanchi *et al*., 2004). p16 was moderately induced in all cell lines at day 1. E7 and E6E7 cells, that express per se high endogenous p16 levels, retained these increased expression levels. In contrast, p16 induction was decreased in epoxomicin-treated CON and E6 cells while $p105^{Rb}$ protein expression levels increased, in accordance with previous studies (Ohtani *et al*., 2004). In conclusion, partial proteasome inhibition triggers a common immediate cellular response in HDFs regardless of their p53 and Rb status.

HDF response to epoxomicin depends on its concentration and the p53/Rb status

As our data highlight that the cellular response to proteasome inhibition depends on the genetic context, and since proteasome inhibitors are currently used as potential antineoplastic drugs (Goldberg, 2007), we conducted a detailed analysis monitoring the response of HDFs to different levels of proteasome inhibition. To this end, epoxomicin concentrations ranging from 5 nM to 50 nM were continuously applied to all cell lines for two or 4 days (see Experimental procedures). The levels of proteasome activity following inhibition were similar in all cell lines for a given epoxomicin concentration, since their relative basal activities were comparable [± 10%; Table 1: CT-L relative activity (%)]. The terminal recorded responses of all treated cell lines are shown in Table 1. When levels of inhibition were about 10% (5 nM of epoxomicin), all cell lines showed few morphological signs of stress, but, as soon as the inhibitor was removed, they continued proliferating normally. Proteasome inhibition by 50% (10 nM epoxomicin) led CON cells to PS, E7 cells to temporary PS followed by crisis/death and E6 and E6E7 cells to eventual resumption of growth. Similar results were obtained for 20 nM epoxomicin (~60% inhibition) except for E7 cells, which died without undergoing growth arrest. Delivery of 30 nM epoxomicin (~70% inhibition) differentially affected only CON cells (as compared to the effects of 20 nM epoxomicin) which were initially growth arrested and then became apoptotic. When inhibition reached ~90% (50 nM epoxomicin) death was dominant in all cell lines, except for E6E7, which resumed growth after approximately 3 weeks. It is also worth noting that resumption of growth in E6E7 cells was considerably faster as compared to other cell lines when we delivered lower (10 nM) epoxomicin concentrations.

Discussion

We have shown in previous studies that partial proteasome inhibition in young HDFs to levels recorded in senescent cells triggers PS (Chondrogianni *et al*., 2003; Chondrogianni & Gonos, 2004). The p53–p21 and the Rb–p16 axes have been shown to act in concert to achieve irreversible growth arrest during RS (Ben-Porath & Weinberg, 2005). Moreover, the same axes have been involved in oxidative stress-mediated PS (Chen *et al*., 1998, 2000a,b, 2002), or in the escape from senescence upon their inactivation (Bond *et al*., 1999; Morris *et al*., 2002). In this study, we have revealed that p53 dictates PS following proteasome inhibition. Rb function is also important for optimal progression but in contrast to p53, its abrogation does not permit a restoration of normal cycling following cessation of proteasome inhibition. Despite a common immediate growth arrest during proteasome inhibition, irreversible PS can only be established in the presence of functional p53.

Previous studies investigating the nature of genes that regulate proliferative lifespan barriers – senescence or mortality stage 1 (M1) and crisis or mortality stage 2 (M2) – have concluded that p53 and Rb axes, through their main effectors, p21 and p16 proteins, are the principal players (Bond *et al*., 1999; Morris *et al*., 2002; Ohtani *et al*., 2004; Shay & Wright, 2005). Cells that manage to overcome these intrinsic cellular controls exhibit an extended lifespan. It is generally accepted that p21 up-regulation triggers the senescence program, while the subsequent p16 accumulation ensures the maintenance and irreversibility of the arrest (Alcorta *et al*., 1996; Stein *et al*., 1999; Morris *et al*., 2002; Beausejour *et al*., 2003). Accordingly, we have also observed an initial p21 induction immediately after epoxomicin treatment in CON cells, followed by a decrease of its levels and a parallel up-regulation of p16.

It has been previously shown that oxidative stress-mediated PS in HDFs is Rb-dependent (Chen *et al*., 2000b), whereas our model reveals a p53 dependence. Apparently these distinct types of stresses and their impacts are multifactorial and differ significantly. Proteasome inhibition enhances not only protein but also DNA and RNA oxidation (Ding *et al*., 2004) and alters mitochondrial homeostasis and turnover (Sullivan *et al*., 2004) in accordance with the effects recorded by oxidants. Nonetheless, many other aspects of cellular function are additionally affected upon proteasome inhibition. These include reversible impairments in protein synthesis per se (Ding *et al*., 2006) and changes in chromatin structure which is characteristic of senescent cells (Ukekawa *et al*., 2004). More importantly, proteasome inhibition deregulates the degradation/cycling of most, if not all, cell cycle regulators resulting in destruction of the fine-tuning of cell cycle progression. For example, we have observed that, although

PCNA RNA expression levels decreased following epoxomicin treatment, the protein levels increased. This could result in continuous signalling for S phase progression even in a time frame where it is not normally scheduled. Collectively, the effects of proteasome inhibition on cell fate are multidimensional, as opposed to the rather distinct outcomes of oxidants. Thus, proteasome inhibition-mediated PS seems to differ significantly from oxidative stress-mediated PS. Nonetheless, partial ROS dependency also occurs, especially during the late steps of establishment of proteasome inhibition-mediated PS.

Despite the differences in the final fate of each epoxomicin-treated cell line, the common immediate response was a G2/M phase arrest followed by moderately elevated rates of apoptosis. This shift is in agreement with the G2/M arrest observed in yeast after delivery of PS-341 proteasome inhibitor (Fleming *et al.*, 2002), mainly mediated by GADD45α and GADD153 proteins (members of the Growth Arrest and DNA Damage-inducible family that has been extensively linked to growth arrest; Hollander & Fornace, 2002). More importantly, GADD153 has been previously shown to be induced upon proteasome inhibition (Zimmermann *et al.*, 2000) as well as upon ER stress (Oyadomari & Mori, 2004). Finally, proteasome inhibition has been correlated to ER stress (Patil & Walter, 2001), which has been recently reported to trigger a transient G2/M arrest in yeast (Bonilla & Cunningham, 2003). Fully consistent with these studies, we have revealed ER stress, GADD153 induction and G2/M arrest in all cell lines. These findings highlight that the immediate cell responses to proteasome inhibition are common and p53/Rb independent.

This study also sheds light on the magnitude of the tight regulation of proteasome-mediated degradation for the cell cycle fine-tuning (Reed, 2006). For example, p27 was up-regulated at the end of treatment (Epox/4d+0), coinciding with the essential absence of S phase CON and E7 cells, or the reduced S phase E6 and E6E7 cells. p27 has been reported to inhibit S phase progression via inactivation of cyclin E-cdk2 complexes (Sherr & Roberts, 2004). p21 was also increased, further inhibiting S phase progression (el-Deiry, 1998). During the recovery period, p16 accumulation probably imposed blockage of cell cycle progression. These two former examples further support the crucial role of p21 and p16 proteins in the regulation of proteasome inhibition-mediated PS. An inverse correlation between GADD153 and p16 could explain the initial down-regulation of p16 RNA levels since GADD153 is a dominant negative inhibitor of C/EBP factors (Oyadomari & Mori, 2004) that have been implicated in p16 expression control (Milde-Langosch *et al.*, 2003). Finally, our results are in marked agreement with microarray analysis data of multiple myeloma cells treated with PS-341 proteasome inhibitor. In this model, proteasome inhibition induced down-regulation of bcl-2, cyclin A, cdk1 and PCNA and up-regulation of GADD and p21 genes (Mitsiades *et al.*, 2002).

Collectively, our results are summarized in Fig. 8. During partial proteasome inhibition, the degradation of key molecules is partially and temporarily restricted and this may result, among other effects, in cell cycle deregulation. Proteasome inhibition also causes ER stress, probably resulting in the Unfolded Protein Response (UPR; Patil & Walter, 2001) that induces the UPR target, GADD153 and leads to G2/M arrest and apoptosis, possibly through disruption of redox homeostasis (Oyadomari & Mori, 2004). These effects are further enhanced in cell lines with intact p53, like CON and E7 cells. In these cells, p53 accumulation is primarily a direct consequence of proteasome inhibition due to its deregulated degradation (Vousden & Lane, 2007) that may be further aggravated by ER stress and UPR induction. Elevated p53 levels result in p21 induction with consequent G1/S arrest (el-Deiry, 1998) and may also dictate G2/M arrest through down-regulation of mitosis-promoting complexes or accumulation of inactive p21-cyclin B1-cdk1 complexes (Taylor *et al.*, 1999). p53 also affects the apoptotic pathway through regulation of pro-apoptotic bax and anti-apoptotic bcl-2 (Vousden & Lane, 2007). In conclusion, it is clear that once the proteasome is partially inhibited, the immediate stress response of all cell lines is common with a clear preference for growth arrest followed by increased death rates.

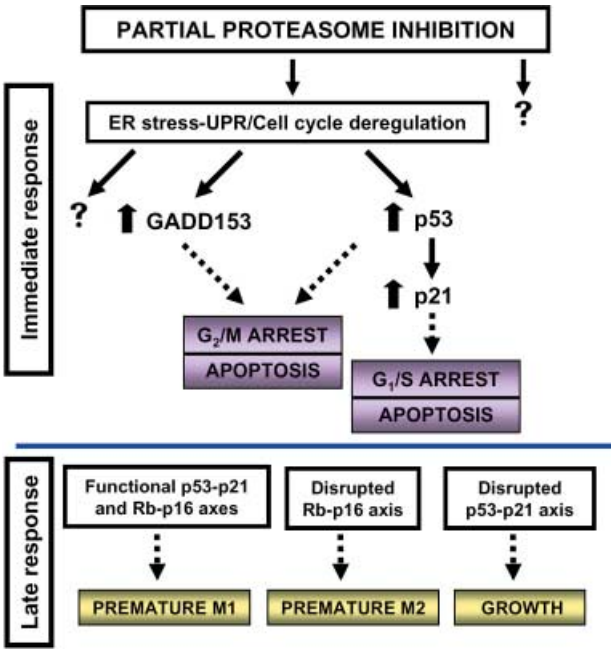

Fig. 8 Model summarizing the HDFs responses to partial proteasome inhibition. Partial proteasome inhibition induces abnormalities in protein degradation and consequently cell cycle deregulation. ER stress and Unfolded Protein Response (UPR) are also induced resulting, among other effects in the induction of the UPR target, GADD153, which in turn leads to G2/M arrest and apoptosis. In cell lines with intact p53, like CON and E7 cells, p53 accumulates resulting in p21 induction that leads to G1/S arrest and apoptosis. Accumulation of p53 may further dictate G2/M arrest. After epoxomicin withdrawal, cell lines with functional p53-p21 and Rb-p16 axes reach to premature M1, cell lines with disrupted Rb-p16 axis exhibit premature M2, and cell lines with disrupted p53-p21 axis resume growth. Solid and dashed arrows indicate direct and indirect reported molecular pathways, respectively; the intermediate steps are not shown and only the end stages are illustrated. Thick arrows (↑) show up-regulation of protein expression. Question marks (**?**) depict other putative pathways.

Following epoxomicin removal, cell lines with both p53-p21 and Rb-p16 intact axes can initialize (via p21 up-regulation), maintain and stabilize (via p16 up-regulation) a typical premature senescence state with permanent G1/S and/or G2/M arrest (Alcorta *et al*., 1996; Stein *et al*., 1999). We suggest that this cellular state represents a premature M1 stage (accelerated senescence). Cell lines that lack Rb but possess over-expressed p53, can up-regulate p21 protein and, thus, initialize a program of accelerated senescence in response to partial proteasome inhibition. However, due to lack of functional Rb-p16 axis (Alcorta *et al*., 1996; Stein *et al*., 1999), this cellular state cannot be maintained and the cells end up dying due to high p53 expression levels (Chen *et al*., 1998). This program is an accelerated M2 stage (premature crisis) characterized by cell loss and increased death rates, normally exhibited by E7-infected primary cells after several weeks of passaging (Bond *et al*., 1999). The similarities in cell cycle distribution profiles between replicative senescent and epoxomicin-treated E7 cells further strengthen this hypothesis. Finally, E6 cells (and E6E7 cells) with defective p53 cannot induce p21 expression following partial proteasome inhibition, thus failing to initiate the program of accelerated senescence. Therefore, they overcome the barrier of senescence initialization and they resume growth. In conclusion, we suggest that if there is a permissive genetic background for senescence initiation/progression, human cells execute an accelerated version of their 'lifespan program' upon partial proteasome inhibition.

Proteasome inhibitors are currently in preclinical trials against various malignancies and tumors (Goldberg, 2007). Our study emphasizes that caution should be exercised in considering the molecular characteristics of each individual cancer type before proteasome inhibitors administration. The eventual cell response depends on the extent of proteasome activity inhibition and, more importantly, it is absolutely linked to the genetic context. Specifically, low levels of inhibition (≤ 10%) almost do not affect any of the cell lines tested, as cultures keep proliferating. Proteasome inhibition between 40% and 60% triggers a wide range of different outcomes, varying from growth arrest/PS and crisis/death to resumption of growth. However, what is even more remarkable is that for inhibition higher than 90%, cells that lack p53 and Rb family proteins are refractory to cell cycle arrest, eventually achieving restoration of normal proliferative status. This pilot analysis straightens out the notion that proteasome inhibition is not a single panacea even for those cell types that are inhibitor-responsive. Although the initial cellular response can be promising, the ultimate outcome can be equally disillusioning. On the promising side, if the genetic context is permissive, lower concentrations of proteasome inhibitors can be delivered to kill the target cells by apoptosis with the concurrent escape of the 'innocent' normal cells from death. Nonetheless, these cells will still have to pay the price of PS.

Senescence is a multifactorial process governed by both genetic and environmental factors that eventually lead to failure of homeostasis. Proteasomal degradation plays a critical role in cellular maintenance. Proteasome expression is altered during aging and RS (Chondrogianni & Gonos, 2005), while its activation confers lifespan extension in primary HDFs (Chondrogianni *et al*., 2005). Here we show that partial proteasome inhibition induces PS (Chondrogianni *et al*., 2003; Chondrogianni & Gonos, 2004) via the p53 pathway. An irregularity in proteasome degradation triggers a cascade of molecular events that can change the cell fate. Thus, it is not absurd to suggest that the proteasome may exert a more pivotal role in the progression of senescence apart from the already exhibited one, mainly based on the insufficient degradation of 'protein waste' like lipofuscin, ceroid or oxidized proteins. It would not be astonishing if alterations in the degradation efficiency of senescence related proteins were revealed in the near future. Anti-aging strategies should not exclusively aim on the transcriptional regulation of key molecules but also on the regulation of their protein turnover.

Experimental procedures

Reagents and antibodies

Epoxomicin was purchased from BIOMOL Research Products Ltd (Exeter, UK). Primary antibodies against bax (sc493; 23 kDa), bcl-2 (sc509; 26 kDa), cyclin A (sc751; 60 kDa), cyclin B1 (sc245; 55 kDa), cdk1 (sc 8395; 34 kDa), GADD45α (sc797; 18 kDa), GADD153 (sc793; 30 kDa), GRP78/BiP (sc1050; 78 kDa), PARP (sc7150; 116/85 kDa), p53 (sc126; 53 kDa), p16 (sc467; 16 kDa), p21 (sc817; 21 kDa), p27 (sc528; 27 kDa), PCNA (sc9857; 36 kDa), GAPDH (sc25778; 37 kDa) and secondary antibodies were purchased from Santa Cruz Biotechnology (Santa Cruz, CA, USA). Primary antibody against $p105^{Rb}$ (554136; 110 kDa) was purchased from BD Pharmingen (San Diego, CA, USA).

Cell lines and culture conditions

IMR90 HDFs (European Collection of Cell Cultures) were infected with HPV16 E6 and/or E7 retroviral constructs as well as with empty vector (pLXSN) as previously described (Chen *et al*., 1998). MDAH041, a p53-null fibroblast cell line and TR9-7 cells, a derivative clone that in the presence of 1 μg mL^{-1} tetracycline (TET^+) does not express p53 protein whereas upon tetracycline removal (TET^-) expresses p53, were a generous gift of Drs G. R. Stark and M. L. Agarwal (Agarwal *et al*., 1995). All cell lines were maintained in DMEM as previously described (Chondrogianni *et al*., 2003). Cells were fed approximately 16 h prior to each assay and cell number was determined in triplicates using a Coulter Z2 counter (Beckman Coulter, Fullerton, CA, USA). Cells were subcultured upon confluence at a split ratio 1 : 2, until they entered senescence.

Cell treatment with epoxomicin and/or NAC

Cells (2×10^5) were seeded in triplicates, fed the following day and 24 h later they were treated with 10 nM epoxomicin or an equal amount of the solvent (DMSO) in the presence of complete medium (with or without tetracycline for TR9-7 cells)

continuously for up to 4 days. Fresh inhibitor was added every day to exclude the possibility of its inactivation at 37 °C. Cultures were exposed to epoxomicin for 24 h (1 day), 48 h (2 days), 72 h (3 days) and 96 h (4 days). Cells were then washed thoroughly with PBS and were either immediately used without recovery (Epox/4d+0) or maintained in complete medium for an additional period of 1 (Epox/4d+1wk), 2 (Epox/4d+2wk) or 3 (Epox/4d+3wk) weeks depending on the cell line and the performed assays. For co-incubation with the antioxidant NAC, 2 mM NAC were added in the cultures for the appropriate time periods. To titrate the effects of epoxomicin in HDFs, cells were treated continuously with 5, 10 and 20 nM of the inhibitor for 4 days or with 30 and 50 nM for 2 days. Cells were then maintained in complete medium and the phenotypic changes were recorded for an additional period of up to 6 weeks.

Cell cycle analysis

Adherent cells were harvested, washed in ice-cold PBS, fixed in 50% (v/v) EtOH and stained with propidium iodide (50 μg mL^{-1}) solution containing 10 μg mL^{-1} RNase. Flow cytometric analysis was performed in a FACS-Calibur flow cytometer equipped with a Modfit software program (Becton-Dickinson, Franklin Lakes, NJ, USA).

RNA extraction and real-time PCR analysis

Total RNA was extracted by using TRIZOL (Invitrogen, Carlsbad, CA, USA) and converted into cDNA by using iScript cDNA synthesis kit (Bio-Rad Laboratories, Hercules, CA, USA). Real-time PCRs were performed in triplicates on an iCycler iQ Real-Time PCR Detection System with iQ SYBR Green Supermix and gene expression analysis was performed with Gene Expression Macro™ Version 1.1 (Bio-Rad Laboratories). Real-time PCR primers used were: p16-R: 5′-AGT CGA CAG CTT CCG GAG G-3′, p16-F: 5′-CTC ACG CCC TAA GCG CA-3′, PCNA-R: 5′-CAA AGA GAC GTG GGA CGA GT-3′, PCNA-F: 5′-AGG TGT TGG AGG CAC TCA AG-3′. GAPDH was used as a normalizer.

Immunoblot analysis

Cells were harvested at indicated time points, lysed in non-reducing Laemmli buffer and proteins were fractionated by SDS-PAGE according to standard procedures (Harlow & Lane, 1999). Proteins were then transferred to nitrocellulose membranes for probing with appropriate antibodies. Secondary antibodies conjugated with horseradish peroxidase and enhanced chemiluminescence were used to detect the bound primary antibodies. Equal protein loading was verified by reprobing each membrane with a GAPDH antibody.

Measurement of ROS

2′,7′-dichlorodihydrofluorescein diacetate (H_2DCFDA, Molecular Probes, Invitrogen, Carlsbad, CA, USA) was used for ROS detection. Cells (10^5) were resuspended in prewarmed PBS ± the dye at a final concentration of 10 μM (loading buffer) and incubated at 37 °C for 30 min. Cells were then resuspended in prewarmed complete medium and incubated at 37 °C for 5 min. The absorption and the emission of the oxidation product were measured at 493 and 520 nm, respectively. Each sample was measured in quadruplicates.

Statistical analysis

Statistics were performed by using Microsoft Excel software. Statistical significance was evaluated using the one-way analysis of variance (ANOVA). Results at $p < 0.05$ or $p < 0.01$ are denoted in graphs by a single or double asterisk, respectively. All values were reported as mean of three independent experiments ± standard error, unless otherwise indicated.

Acknowledgments

We are grateful to Drs Agarwal and Stark for cell lines. This work was supported by a European Union Integrated Project/FP-6 grant ('Proteomage', LSHM-CT-518230) to ESG.

References

Agarwal ML, Agarwal A, Taylor WR, Stark GR (1995) p53 controls both the G2/M and the G1 cell cycle checkpoints and mediates reversible growth arrest in human fibroblasts. *Proc. Natl Acad. Sci. USA* **92**, 8493–8497.

Alcorta DA, Xiong Y, Phelps D, Hannon G, Beach D, Barett JC (1996) Involvement of the cyclin-dependent kinase inhibitor p16 (INK4a) in replicative senescence of normal human fibroblasts. *Proc. Natl Acad. Sci. USA* **93**, 13742–13747.

Barradas M, Gonos ES, Zebedee Z, Kolettas E, Petropoulou C, Delgado MD, Leon J, Hara E, Serrano M (2002) Identification of a candidate tumor-suppressor gene specifically activated during Ras-induced senescence. *Exp. Cell Res.* **273**, 127–137.

Beausejour CM, Krtolica A, Galimi F, Narita M, Lowe SW, Yaswen P, Campisi J (2003) Reversal of human cellular senescence: roles of the p53 and p16 pathways. *EMBO J.* **22**, 4212–4222.

Ben-Porath I, Weinberg RA (2005) The signals and pathways activating cellular senescence. *Int. J. Biochem. Cell Biol.* **37**, 961–976.

Bond JA, Haughton MF, Rowson JM, Smith PJ, Gire V, Wynford-Thomas D, Wyllie FS (1999) Control of replicative life span in human cells: barriers to clonal expansion intermediate between M1 senescence and M2 crisis. *Mol. Cell. Biol.* **19**, 3103–3114.

Bonilla M, Cunningham KW (2003) Mitogen-activated protein kinase stimulation of Ca(2+) signalling is required for survival of endoplasmic reticulum stress in yeast. *Mol. Cell. Biol.* **14**, 4296–4305.

Chen QM, Bartholomew JC, Campisi J, Acosta M, Reagan JD, Ames BN (1998) Molecular analysis of H_2O_2-induced senescent-like growth arrest in normal human fibroblasts: p53 and Rb control G1 arrest but not cell replication. *Biochem. J.* **332**, 143–150.

Chen QM, Liu J, Merrett JB (2000a) Apoptosis or senescence-like growth arrest: influence of cell-cycle position, p53, 21 and bax in H2O2 response of normal human fibroblasts. *Biochem. J.* **347**, 543–551.

Chen QM, Tu VC, Catania J, Burton M, Toussaint O, Dilley T (2000b) Involvement of Rb family proteins, focal adhesion proteins and protein

synthesis in senescent morphogenesis induced by hydrogen peroxide. *J. Cell Sci*. **113**, 4087–4097.

Chen QM, Merrett JB, Dilley T, Purdom S (2002) Down regulation of p53 with HPV E6 delays and modifies cell death in oxidant response of human diploid fibroblasts: an apoptosis-like cell death associated with mitosis. *Oncogene* **21**, 5313–5324.

Chondrogianni N, Gonos ES (2004) Proteasome inhibition induces a senescence-like phenotype in primary human fibroblasts cultures. *Biogerontology* **5**, 55–61.

Chondrogianni N, Gonos ES (2005) Proteasome dysfunction in mammalian aging: steps and factors involved. *Exp. Gerontol*. **40**, 931–938.

Chondrogianni N, Stratford FLL, Trougakos IP, Friguet B, Rivett AJ, Gonos ES (2003) Central role of the proteasome in senescence and survival of human fibroblasts: induction of a senescence-like phenotype upon its inhibition and resistance to stress upon its activation. *J. Biol. Chem*. **278**, 28026–28037.

Chondrogianni N, Tzavelas C, Pemberton AJ, Nezis IP, Rivett AJ, Gonos ES (2005) Overexpression of proteasome β_5 subunit increases the amount of assembled proteasome and confers ameliorated response to oxidative stress and higher survival rates. *J. Biol. Chem*. **280**, 11840–11850.

Ciechanover A (2005) Intracellular protein degradation: from a vague idea thru the lysosome and the ubiquitin-proteasome system and onto human diseases and drug targeting. *Cell Death Differ*. **12**, 1178–1190.

Collado M, Blasco MA, Serrano M (2007) Cellular senescence in cancer and aging. *Cell* **130**, 223–233.

el-Deiry WS (1998) Regulation of p53 downstream genes. *Semin. Cancer Biol*. **8**, 345–357.

Di Micco R, Fumagalli M, Cicalese A, Piccinin S, Gasparini P, Luise C, Schurra C, Garre M, Nuciforo PG, Bensimon A, Maestro R, Pelicci PG, d'Adda di Fagagna F (2006) Oncogene-induced senescence is a DNA damage response triggered by DNA hyper-replication. *Nature* **444**, 638–642.

Ding Q, Dimayuga E, Merkesbery WR, Keller JN (2004) Proteasome inhibition increases DNA and RNA oxidation in astrocyte and neuron cultures. *J. Neurochem*. **91**, 1211–1218.

Ding Q, Dimayuga E, Merkesbery WR, Keller JN (2006) Proteasome inhibition induces reversible impairments in protein synthesis. *FASEB J*. **20**, 1055–1063.

Fleming JA, Lightcap ES, Sadis S, Thoroddsen V, Bulawa CE, Blackman RH (2002) Complementary whole-genome technologies reveal the cellular response to proteasome inhibition by PS-341. *Proc. Natl Acad. Sci. USA* **99**, 1461–1466.

Goldberg AL (2007) Functions of the proteasome: from protein degradation and immune surveillance to cancer therapy. *Biochem. Soc. Trans*. **35**, 12–17.

Harlow E, Lane D (1999) *Using Antibodies: A Laboratory Manual*. Cold Spring Harbor, NY: Cold Spring Harbor Laboratory Press.

Hollander MC, Fornace AJ Jr (2002) Genomic instability, centrosome amplification, cell cycle checkpoints and GADD45a. *Oncogene* **21**, 6228–6233.

Khidr L, Chen PL (2006) Rb, the conductor that orchestrates life, death and differentiation. *Oncogene* **25**, 5210–5219.

Kikuchi S, Shinpo K, Takeuchi M, Yamagishi S, Makita Z, Sasaki N, Tashiro K (2003) Glycation: a sweet tempter for neuronal death. *Brain Res. Rev*. **41**, 306–323.

Lavin MF, Gueven N (2006) The complexity of p53 stabilization and activation. *Cell Death Differ*. **13**, 941–950.

Malanchi I, Accardi R, Diehl F, Smet A, Androphy E, Hoheisel J, Tommasino M (2004) Human papillomavirus type 16 E6 promotes retinoblastoma protein phosphorylation and cell cycle progression. *J. Virol*. **78**, 13769–13778.

Milde-Langosch K, Loning T, Bamberger A-M (2003) Expression of the CCAAT/enhancer-binding proteins C/EBPα, C/EBPβ and C/EBPδ in breast cancer: correlations with clinicopathologic parameters and cell-cycle regulatory proteins. *Breast Cancer Res. Treat*. **79**, 175–185.

Mitsiades N, Mitsiades CS, Poulaki V, Chaudan D, Fanourakis G, Gu X, Bailey C, Joseph M, Libermann TA, Treon SP, Munshi NC, Richardson PG, Hideshima T, Anderson KC (2002) Molecular sequelae of proteasome inhibition in human multiple myeloma cells. *Proc. Natl Acad. Sci. USA* **99**, 14374–14379.

Morris M, Hepburn P, Wynford-Thomas D (2002) Sequential extension of proliferative lifespan in human fibroblasts induced by overexpression of CDK4 or 6 and loss of p53 function. *Oncogene* **21**, 4277–4288.

Münger K, Howley PM (2002) Human papillomavirus immortalization and transformation functions. *Virus Res*. **89**, 213–228.

Ohtani N, Yamakoshi K, Takahashi A, Hara E (2004) The p16INK4a-RB pathway: molecular link between cellular senescence and tumor suppression. *J. Med. Invest*. **51**, 146–153.

Oren M (2003) Decision making by p53: life, death and cancer. *Cell Death Differ*. **10**, 431–442.

Oyadomari S, Mori M (2004) Roles of CHOP/GADD153 in endoplasmic reticulum stress. *Cell Death Differ*. **11**, 381–389.

Patil C, Walter P (2001) Intracellular signaling from the endoplasmic reticulum to the nucleus: the unfolded protein response in yeast and mammals. *Curr. Opin. Cell Biol*. **13**, 349–355.

Reed SI (2006) The ubiquitin-proteasome pathway in cell cycle control. *Results Probl. Cell Differ*. **42**, 147–181.

Serrano M, Lin AW, McCurrach ME, Beach D, Lowe SW (1997) Oncogenic ras provokes premature cell senescence associated with accumulation of p53 and p16INK4a. *Cell* **88**, 593–602.

Shay JW, Wright WE (2005) Senescence and immortalization: role of telomeres and telomerase. *Carcinogenesis* **26**, 867–874.

Sherr CJ, Roberts JM (2004) Living with or without cyclins and cyclin-dependent kinases. *Genes Dev*. **18**, 2699–2711.

Stein GH, Drullinger LF, Soulard A, Dulic V (1999) Differential roles for cyclin-dependent kinase inhibitors p21 and p16 in the mechanisms of senescence and differentiation in human fibroblasts. *Mol. Cell. Biol*. **19**, 2109–2117.

Sullivan PG, Dragicevic NB, Deng JH, Bai Y, Dimayuga E, Ding O, Chen Q, Bruce-Keller AJ, Keller JN (2004) Proteasome inhibition alters neural mitochondrial homeostasis and mitochondria turnover. *J. Biol. Chem*. **279**, 20699–20707.

Taylor WR, DePrimo SE, Agarwal A, Agarwal ML, Scholthal AH, Katula KS, Stark GR (1999) Mechanisms of G2 arrest in response to overexpression of p53. *Mol. Biol. Cell*. **10**, 3607–3622.

Ukekawa R, Maegawa N, Mizutani E, Fujii M, Ayusawa D (2004) Proteasome inhibitors induce changes in chromatin structure characteristic of senescent human fibroblasts. *Biosci. Biotechnol. Biochem*. **68**, 2395–2397.

Vousden KH, Lane DP (2007) p53 in health and disease. *Nat. Rev. Mol. Cell Biol*. **8**, 275–283.

Wojcik C (1999) Proteasomes in apoptosis: villains or guardians? *Cell Mol. Life Sci*. **56**, 908–917.

Zimmermann J, Erdmann D, Lalande I, Grossenbacher R, Noorani M, Furst P (2000) Proteasome inhibitor induced gene expression profiles reveal overexpression of transcriptional regulators ATF3, GADD153 and MAD1. *Oncogene* **19**, 2913–2920.

Supporting Information

Additional supporting information may be found in the online version of this article.

Appendix S1 Supplementary experimental procedures.

Fig. S1 Protein expression levels of proteasome subunits and levels of oxidized proteins in CON, E7, E6 and E6E7 cells. Immunoblot analysis of β2, β5 and α7 proteasome subunits as well as oxidized proteins in CON, E7, E6 and E6E7 cells. Equal protein loading was verified by reprobing the membranes with a GAPDH antibody (lower panel).

Fig. S2 Protein expression levels of phosphorylated p38 and p53 in CON, E7, E6 and E6E7 cells following partial proteasome inhibition. Immunoblot analysis of phosphorylated p53 on Ser 15 and phosphorylated p38 on Tyr 182 in CON, E7, E6 and E6E7 cells exposed to 10 nM epoxomicin or DMSO immediately (4d+0), one (4d+1wk) and two (4d+2wk) weeks after inhibitor removal. Equal protein loading was verified by reprobing the membranes with a GAPDH antibody.

Please note: Wiley-Blackwell are not responsible for the content or functionality of any supporting information supplied by the authors. Any queries (other than missing material) should be directed to the *Aging Cell* Central Office.